

RESEARCH ARTICLE

White matter microstructure disruption in early stage amyloid pathology

Lyduine E. Collij¹ | Silvia Ingala¹ | Herwin Top¹ | Viktor Wottschel¹ |
 Kristine E. Stickney² | Jori Tomassen³ | Elles Konijnenberg³ | Mara ten Kate¹ |
 Carole Sudre^{3,4} | Isadora Lopes Alves¹ | Maqsood M. Yaqub¹ | Alle Meije Wink¹ |
 Dennis Van 't Ent² | Philip Scheltens³ | Bart N.M. van Berckel¹ |
 Pieter Jelle Visser^{3,5,6} | Frederik Barkhof^{1,4} | Anouk Den Braber^{2,3}

¹ Dept. of Radiology and Nuclear Medicine, Amsterdam UMC, Location VUmc, Amsterdam, The Netherlands

² Dept. of Biological Psychology, VU University Amsterdam, Amsterdam, The Netherlands

³ Alzheimer Center, Amsterdam UMC, Location VUmc, Amsterdam, The Netherlands

⁴ Institute of Neurology and Healthcare Engineering, University College London, London, UK

⁵ Department of Psychiatry and Neuropsychology, School for Mental Health and Neuroscience (MHeNS), Alzheimer Centrum Limburg, Maastricht University, Maastricht, The Netherlands

⁶ Department of Neurobiology, Care Sciences Division of Neurogeriatrics, Karolinska Institutet, Stockholm, Sweden

Correspondence

Lyduine Collij, Radiology and Nuclear Medicine, Amsterdam UMC, Location VUmc, PK-1x014, Boelelaan 1117, 1081 HV Amsterdam, The Netherlands.

Email: l.collij@amsterdamumc.nl

Abstract

Introduction: Amyloid beta (A β) accumulation is the first pathological hallmark of Alzheimer's disease (AD), and it is associated with altered white matter (WM) microstructure. We aimed to investigate this relationship at a regional level in a cognitively unimpaired cohort.

Methods: We included 179 individuals from the European Medical Information Framework for AD (EMIF-AD) preclinAD study, who underwent diffusion magnetic resonance (MR) to determine tract-level fractional anisotropy (FA); mean, radial, and axial diffusivity (MD/RD/AxD); and dynamic [¹⁸F]flutemetamol positron emission tomography (PET) imaging to assess amyloid burden.

Results: Regression analyses showed a non-linear relationship between regional amyloid burden and WM microstructure. Low amyloid burden was associated with increased FA and decreased MD/RD/AxD, followed by decreased FA and increased MD/RD/AxD upon higher amyloid burden. The strongest association was observed between amyloid burden in the precuneus and body of the corpus callosum (CC) FA and diffusivity (MD/RD) measures. In addition, amyloid burden in the anterior cingulate cortex strongly related to AxD and RD measures in the genu CC.

Discussion: Early amyloid deposition is associated with changes in WM microstructure. The non-linear relationship might reflect multiple stages of axonal damage.

KEYWORDS

Amyloid beta (A β), diffusion tensor imaging (DTI), magnetic resonance imaging (MRI), positron emission tomography (PET), preclinical Alzheimer's disease (AD), white matter microstructure

1 | INTRODUCTION

Amyloid beta (A β) plaque accumulation is a pathological hallmark of Alzheimer's disease (AD), and has been associated with alterations in

white matter (WM) microstructure,^{1,2} with the first being quantified in vivo by positron emission tomography (PET) and the latter measured on magnetic resonance imaging (MRI) using diffusion tensor imaging (DTI). However, reports regarding the relationship between amyloid

This is an open access article under the terms of the [Creative Commons Attribution-NonCommercial-NoDerivs](https://creativecommons.org/licenses/by-nc-nd/4.0/) License, which permits use and distribution in any medium, provided the original work is properly cited, the use is non-commercial and no modifications or adaptations are made.

© 2021 The Authors. *Alzheimer's & Dementia: Diagnosis, Assessment & Disease Monitoring* published by Wiley Periodicals, LLC on behalf of Alzheimer's Association

accumulation and disruption in WM microstructure show conflicting results.

Preclinical AD subjects have been reported to show loss of WM tract integrity, that is, decrease of fractional anisotropy (FA) and increase of mean diffusivity (MD), compared to amyloid-negative controls.³⁻⁵ Of interest, the tracts with the most pronounced WM alterations (corpus callosum, fornix, superior longitudinal fasciculi, and cingulum)^{3,6,7} are anatomically connected to early amyloid-affected regions,⁸⁻¹¹ suggesting that WM alterations may be driven by amyloid deposition. However, the opposite relationship has also been reported, with higher FA in the high amyloid group compared to the amyloid-negative group.⁷ More recent work could reconcile previous conflicting reports because a non-linear relationship between global measures of amyloid burden and DTI has been observed.^{3,12}

These inconsistencies could also be due to the challenges of detecting early amyloid pathology in the preclinical stages of AD.¹¹ Because amyloid burden is often low or focal in this population, global assessment and dichotomization of standardized uptake value ratios (SUVs) are likely suboptimal and indeed have been demonstrated to miss the earliest signs of A β pathology.^{13,14} Full quantification and regional investigations could provide more sensitive A β measurements in this population,^{9,15,16} thereby better enabling the assessment of the relationship between amyloid burden and WM microstructure.

This study aimed to assess the relation between early stage amyloid burden and WM-tract microstructure alterations in cognitively unimpaired subjects using global and regional DTI measures and quantitative global and regional amyloid burden derived from dynamic [¹⁸F]flutemetamol PET imaging.

2 | METHODS

2.1 | Cohort

The data used in this study originate from the Innovative Medicines Initiative (IMI) European Medical Information Framework for AD (EMIF-AD) project (<http://www.emif.eu/>). The overall aim of the EMIF-AD project is to discover and validate diagnostic markers, prognostic markers, and risk factors for AD in non-demented subjects.

2.2 | Subjects

A total of 199 subjects from the EMIF PreclinAD cohort were included at the VU University Medical Center, after being referred by The Netherlands Twin Register.¹⁷ Inclusion criteria were age ≥ 60 years and normal cognition according to a delayed recall score of > -1.5 standard deviation (SD) of demographically adjusted normative data on the Consortium to Establish a Registry for Alzheimer's Disease (CERAD) 10-word list, a Telephone Interview for Cognitive Status modified (TICS-m) score of 23 or higher, a 15-item Geriatric Depression Scale (GDS) score of < 11 , and a Clinical Dementia Rating (CDR) scale score of zero. Exclusion criteria were the presence of any phys-

RESEARCH IN CONTEXT

- 1. Systematic review:** Literature was reviewed using traditional sources (eg, PubMed). Although a loss of white matter (WM) integrity has been clearly described in clinical Alzheimer's disease (AD), recent work suggests a more complex relationship between amyloid burden and WM microstructural changes in its preclinical stages. The most relevant and latest papers are cited in this work.
- 2. Interpretation:** Our findings in a cognitively unimpaired population support the association between early amyloid burden and disrupted WM microstructure as measured by diffusion tensor imaging (DTI) analysis. The apparent non-linear relationship between these two measures might reflect initial amyloid-associated compensatory mechanisms of the WM, followed by axonal degeneration.
- 3. Future directions:** This work highlights the importance of complementary multi-modal imaging approaches in the context of preclinical AD. Understanding the relationship between amyloid accumulation and subsequent brain changes could improve risk-profiling efforts, and possibly support targeted inclusion for secondary prevention trials. Longitudinal validation of these findings is necessary.

ical, neurological, or psychiatric condition that might interfere with cognitive performance.¹⁸ The Medical Ethics Review Committee of the VU University Medical Center performed approval of the study in Amsterdam. Research was performed according to the principles of the Declaration of Helsinki and in accordance with the Medical Research Involving Human Subjects Act and codes on 'good use' of clinical data and biological samples as developed by the Dutch Federation of Medical Scientific Societies. All participants gave written informed consent.

Dynamic PET acquisition or quantification failed in four and five subjects, respectively. Seven subjects were excluded due to the detection of space-occupying lesions with the characteristics of meningioma, one due to incorrect field of view, and one due to failed DTI quantification, resulting in the final inclusion of 179 subjects.

2.3 | Image acquisition and processing

2.3.1 | PET image acquisition and processing

Dynamic scanning was performed on a Philips Ingenuity TF PET-MRI camera (Philips Healthcare, Cleveland, USA) using the dual-time window acquisition protocol,¹⁹ with 30-minute scans acquired immediately after manual injection (191 ± 20 MBq) of [¹⁸F]flutemetamol.

After a 60-minute break, a second scan of 20 minutes was acquired (90 to 110 minutes post injection). In addition, a dedicated magnetic resonance sequence (attenuation MR) was acquired prior to each PET scan for attenuation correction (AC). The first emission scans were reconstructed in 18 frames with increasing time length, by applying the line-of-response row action maximum likelihood algorithm (LOR-RAMLA) reconstruction algorithm for the brain. The second scan was reconstructed by four frames with 300 seconds each. Images were pre-processed with Vinci Software version 2.56 (<http://vinci.sf.mpg.de/>) to combine the two PET scans into single multi-frame images. Furthermore, the multimodality setting of Vinci was used for co-registration of an individual's T1-weighted MRI sequence to the dynamic scans. Cerebellar gray matter was chosen as the reference tissue. Non-displaceable Binding Potential (BP_{ND}) values were calculated by using the receptor parametric mapping (RPM) implementation of the Simplified Reference Tissue Model (SRTM)²⁰ in PPET software.^{19,21} For analyses, distribution volume ratio (DVR) was calculated as a linear function of receptor availability for radioligand ($BP_{ND} + 1$). The co-registered T1-weighted MR images were warped into Montreal Neurological Institute (MNI) space using Statistical Parametric Mapping (SPM) 12 (<https://www.fil.ion.ucl.ac.uk/spm/>). Subsequently, the subject-specific conversion matrix was used to warp the corresponding PET image into MNI.

Amyloid positivity was visually assessed by three readers who completed the training provided by GE Healthcare.²² For the visual read, image maximum intensity was scaled to 90% of the pons signal using rainbow color scaling, and transverse, sagittal, and coronal views were displayed using the software package Vinci 2.56 and assessed together with a T1-weighted MR scan to assist reading in the presence of atrophy in the visual assessment. Images were rated as either *positive* (binding in one or more cortical brain region or striatum unilaterally) or *negative* (predominantly WM uptake).¹¹

The Desikan-Killiany (DK) atlas²³ was used to extract global and regional cortical DVR values normalized to cerebellar gray matter. Global amyloid burden consisted of the volume-weighted average of 27 cortical regions.²⁴ A cut-off for amyloid positivity was determined using Gaussian mixture modeling, taking the mean and two standard deviations of the left (normal) curve (ie, $DVR \geq 1.15$). Early accumulating regions were selected based on previous work in the amyloid staging field,^{8,9,24-26} which included the anterior cingulate cortex (ACC), posterior cingulate cortex (PCC), isthmus cingulate cortex (ICC), precuneus (PC), insula, and lateral orbitofrontal cortex (IOFC).

2.3.2 | MR image acquisition and processing

Whole-brain scans were obtained using a single 3T MRI scanner (Philips Ingenuity Time-of-Flight PET-MR scanner) with an eight-channel head coil. Isotropic structural three-dimensional (3D) T1-weighted images were acquired using a sagittal turbo field echo sequence (1.00 mm³ isotropic voxels, repetition time = 7.9 ms, echo time = 4.5 ms, and flip angle = 8°), and 3D sagittal fluid-attenuated inversion recovery (FLAIR) sequences (1.12 mm³ isotropic voxels,

repetition time = 4800 ms, echo time = 279 ms, and inversion time = 1650 ms) were acquired for the assessment of white matter hyperintensities (WMHs). All MRI scans were visually assessed by an experienced neuroradiologist for incidental findings.

3D-T1 and FLAIR sequences were used to automatically segment WMHs using a Gaussian mixture model (GMM), accounting for expected (healthy) and outlier observations, which allows for a quantitative measure of WMH volume. A full description of the used framework can be found in Sudre et al. (2015).²⁷ It is notable that WMH volumes were extracted from voxels considered as abnormal using comparisons to the characteristics of healthy WM (Figure S1). A complete description of WMH pathology in this cohort can be found in a previous publication by our group (ten Kate et al., 2018).²⁸

2.3.3 | DTI image acquisition and processing

Images were acquired with a Philips 3T Achieva scanner (EPI sequence repetition time (TR) = 7517 ms, echo time (TE) = 92 ms). Diffusion gradients were collected over 32 non-collinear directions ($b = 1000$ s/mm²). One additional scan per subject with no diffusion weighting ($b = 0$ s/mm²) was acquired. The field of view was 256 × 256 × 112 mm with an acquisition matrix of 128 × 128 mm. Gapless, 2-mm-thick slices were taken. Voxels measured 2 × 2 × 2 mm.

Diffusion images were preprocessed using the Functional Magnetic Resonance Imaging of the Brain (FMRIB) Diffusion Toolbox from FMRIB's Software Library (FSL).²⁹ Images were first skull-stripped using the brain extraction tool (BET) and then corrected for eddy-current distortions with standard settings. The diffusion tensor model was then fitted to independent voxels for fractional anisotropy (FA) and mean diffusivity (MD) measurements. Independent regional measurements of FA and MD data were performed with tract-based spatial statistics (TBSS).³⁰ TBSS was used to select the most typical subject (smallest amount of average warping) from the whole cohort as the target image, which was affine-aligned (warped) to MNI standard space. Subsequently, these transformations were applied to all subjects' FA images, transforming them to MNI standard space. Finally, TBSS was used to project all subjects' FA data onto a mean FA tract skeleton,³⁰ which was then repeated for MD, radial diffusivity (RD), and axial diffusivity (AxD).

Averaged values within the skeleton were used to reflect global DTI metrics of FA, MD, RD, and AxD. In addition, regions of interest (ROIs) as defined by the John Hopkins University (JHU) ICBM-DTI-81 white-matter atlas (<https://fsl.fmrib.ox.ac.uk/fsl/fslwiki/Atlases>)³¹ were applied to the skeletonized DTI data, which is suggested to be preferred when aiming to identify subtle changes in the corpus callosum (CC) and tracts neighboring the ventricles.³² Eight tracts were selected based on previous literature.^{3,6,7} These included the cingulum of the cingulate gyrus (CG); parahippocampal cingulum (PaCi); superior longitudinal fasciculus (SLF); the genu, body, and splenium of the corpus callosum (CC); fornix; and uncinate fasciculus (UF). Projection fibers were excluded because we were interested primarily in intracranial connections.

MD represents the diffusion average, but it provides no information about the direction in which diffusion is increasing or decreasing. Therefore, MD measures were complemented with measures of axial and radial diffusivity, which do take the direction of diffusion into account, and used to determine which measure was most sensitive to amyloid-driven WM disruption.

2.4 | Statistical analyses

Statistical analyses were performed with Statistical Package for the Social Sciences (SPSS) version 26. Generalized estimating equations (GEEs) with an exchangeable working correlation matrix and a robust estimator was applied to all multiple regression models to correct for twin status.³³ Dependent and independent variables were standardized prior to the regression analyses in order to obtain standardized betas. Effect sizes were obtained: R^2 values ≤ 0.010 were considered small, 0.090 medium, and ≥ 0.250 a large effect size. Significance was set at a P -value $< .05$ (Bonferroni correction $P = .006$).

2.4.1 | Assessments of covariates

Regression analyses were performed between global DVR, FA, and MD, correcting for age, sex, and WMH volume. Subsequent analyses were corrected for all covariates showing a significant relationship with either DVR or DTI measures (Figure S2).

2.4.2 | Assessment of amyloid and DTI relationships

First, differences in global FA and MD for amyloid– and amyloid+ subjects were investigated. Then, regression analyses between continuous measures of global and regional amyloid burden and global and tract-specific FA and MD measures were performed. Significant associations between regional amyloid and MD were further investigated for AxD and RD alterations.

Both linear and quadratic fits were applied to the regression models and the best fit was selected using the Quasi-likelihood under the Independence Model Criterion (QIC) parameter, which is the equivalent of the Akaike criterion used in GEE analysis.³⁴ The lowest QIC value was selected; the reported ΔQIC indicates the difference in QIC value between models.

3 | RESULTS

Demographic characteristics of the cohort are shown in Table 1. Results that survived Bonferroni correction are shown in Table 2. Full results can be found in Table S1 and S2.

TABLE 1 Demographics of the cohort

Clinical Characteristics (N = 179)	
Sex (% female)	102 (57%)
Age	70.1 (7.14)
MMSE score	29.0 (1.15)
WMH	5.41E ⁰³ (7.33E ⁰³)
APOE $\epsilon 4$ positivity (%)	74 (41.3%)
Global amyloid DVR	1.03 (0.12)
Global amyloid positivity (%) ^a	25 (14%)

^aBased visual assessment of the parametric amyloid PET images.¹¹ Continuous measures are shown as mean (SD) unless otherwise specified. Abbreviations: MMSE, Mini Mental State Examination; WMH, white matter hyperintensity; DVR, distribution volume ratio.

3.1 | Global amyloid burden and DTI measures

No differences were observed between visually amyloid– or amyloid+ subjects in global white matter (WM) fractional anisotropy (FA) ($P = .12$) or mean diffusivity (MD) ($P = .862$) or between subjects classified as amyloid– or amyloid+ based on their global quantitative amyloid burden (cut-off DVR > 1.15) in global WM FA ($P = .09$) or MD ($P = .88$). When a continuous measure of global amyloid burden is used, a marginal association with global FA, superior longitudinal fasciculus (SLF) FA, but not with global MD was observed.

3.2 | Regional amyloid burden and DTI measures

Significant associations between FA in the body of the corpus callosum (CC) and amyloid burden in the anterior cingulate cortex (ACC), posterior cingulate cortex (PCC), insula, and most strongly the precuneus, were observed. For the precuneus, also a strong association with FA in the splenium of the CC was shown. Finally, amyloid burden in the insula also related to FA in the cingulum. For all associations, an initial higher FA upon an increase in amyloid burden, followed by an inflection point and subsequently lower FA for further increases in amyloid burden was apparent. Indeed, the quadratic model was preferred for all associations according to the quasi information criterion (QIC), as it better described the non-linear trend in the data. The associations with amyloid burden in the precuneus survived Bonferroni-correction (Table 2 and Figure 1).

Next, we tested the associations between MD and amyloid burden. MD and FA showed opposite trends as a function of amyloid burden, as expected in the presence of axonal degeneration. More specifically, significant associations were found between MD in the genu of the CC and amyloid burden in ACC, PCC, ICC, and precuneus. The latter also strongly related to MD in the body of the CC and survived Bonferroni correction. Again, most associations comprised a negative linear and positive quadratic amyloid component, also resulting in a preference for the quadratic model according to QIC (Table 2 and Figure 1).

TABLE 2 Significant associations between amyloid burden and DTI measures

Predictor	Dependent	Model parameters					
		Linear		Quadratic		Model fit	
		β	<i>P</i>	<i>B</i>	<i>p</i>	ΔQIC	R^2
Fractional anisotropy							
DVR precuneus	Body CC	.36	<.001	-.10	.001	8.2	.15
	Splenium CC	.26	.002	-.10	.001	6.0	.08
DVR insula	Cingulum	.23	.005	-.07	.012	3.0	.04
Mean diffusivity							
DVR precuneus	Body CC	-.34	<.001	.12	.001	4.5	.10
Axial diffusivity							
DVR anterior cingulate cortex	Genu CC	-.21	.004	.08	<.001	5.7	.06
Radial diffusivity							
DVR anterior cingulate cortex	Genu CC	-.28	.005	.07	.003	2.4	.03
DVR precuneus	Body CC	-.32	<.001	.09	.004	2.8	.09

GEE results that survived Bonferroni correction are shown adjusted for age, sex, and white matter hyperintensity (WMH). All models included random effect for twin status. Standardized betas are shown, calculated with z-scores. For all analyses, a quadratic model fit was preferred by the quasi information criterion (QIC).

Abbreviations: DVR = distribution volume ratio, CC = corpus callosum.

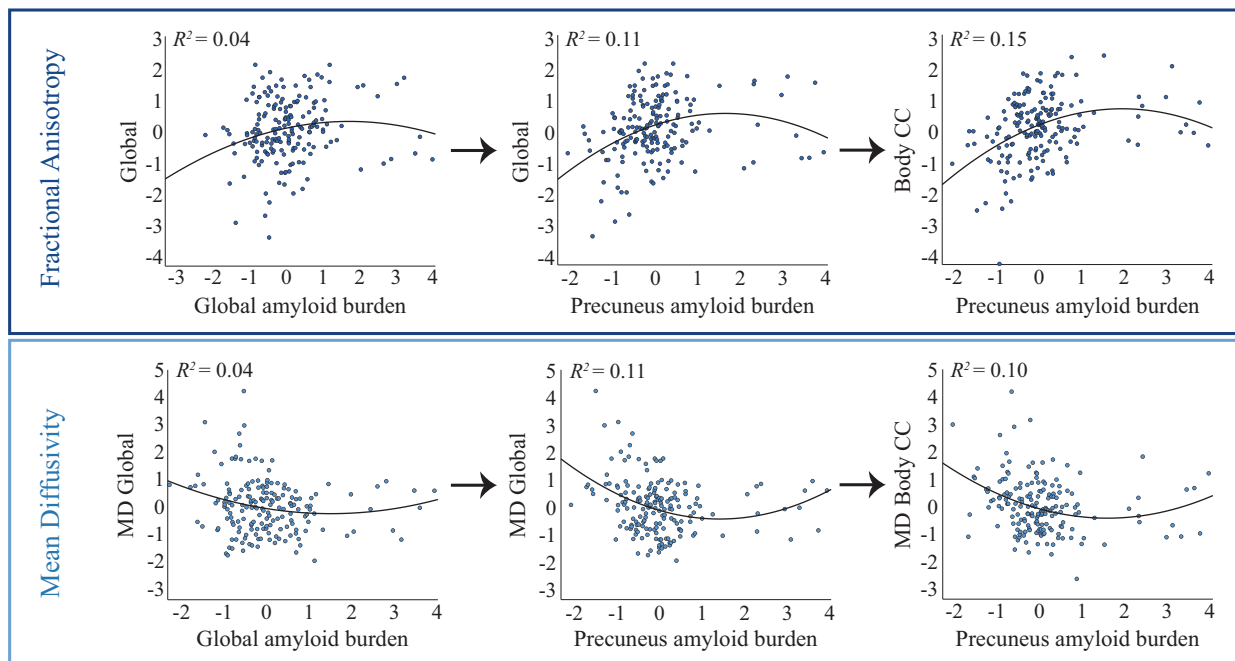


FIGURE 1 Association between amyloid burden and FA/MD. Scatterplots show the associations between standardized amyloid burden (x-axis) and standardized DTI measures (y-axis), corrected for age, sex, and WMH load. Left panels: A significant non-linear relationship was observed between global DVR and global WM FA and no significant relationship was observed between global DVR and global WM MD. Middle panels: A non-linear relationship at trend level was observed between precuneus DVR and FA/MD in the body of the CC. Right panels: A non-linear association was observed between FA/MD of the body CC and amyloid burden in the precuneus, which survived Bonferroni correction

3.3 | Axial and radial diffusivity DTI measures

Finally, significant associations between regional amyloid burden and tract-level MD were further analyzed for underlying axial diffusivity

(AxD) and radial diffusivity (RD) patterns. Both RD and AxD in the genu of the CC strongly related to amyloid burden in the ACC. In addition, the relationship between amyloid burden in the precuneus and diffusivity in the body of the CC was fully explained by RD. All these

Axial and Radial Diffusivity

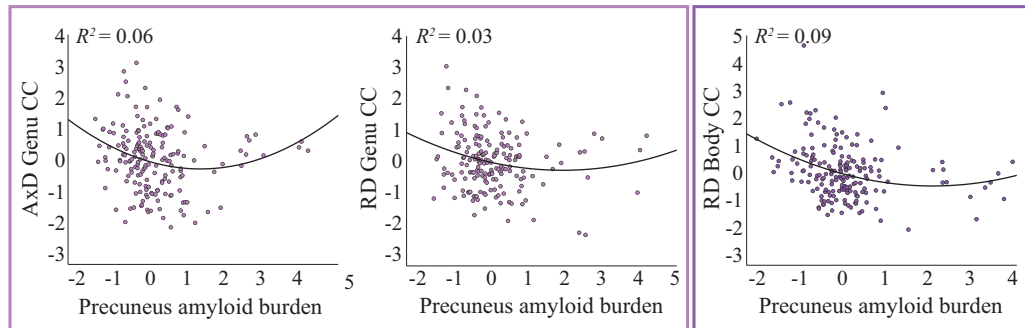


FIGURE 2 Association between amyloid burden and AxD/RD. Scatterplots show the associations between standardized amyloid burden in the precuneus (x-axis) and standardized DTI measures (y-axis), corrected for age, sex, and WMH load. Left/middle panel: A significant non-linear relationship was observed between amyloid burden and AxD/RD in the genu of the corpus callosum (CC). Right panel: A significant non-linear relationship was observed between amyloid burden and RD in the body of the CC

associations survived Bonferroni correction (Table 2) and AxD/RD exhibited a quadratic relationship with amyloid burden similar to that of MD (Figure 2).

4 | DISCUSSION

The current study suggests a non-linear relationship between regional amyloid burden and white matter (WM) microstructural measures in a cognitively unimpaired elderly population. An initial increase in amyloid burden corresponded to higher FA and lower diffusivity measures (MD/AxD/RD), followed, respectively, by a maximum for FA and a minimum for diffusivity measures, and subsequently lower FA and higher diffusivity measures for further increases in amyloid burden. This association was particularly evident between amyloid burden in the precuneus and FA/MD measures in the body of the corpus callosum (CC) and between amyloid burden in the anterior cingulate cortex (ACC) and AxD and RD measures of the genu of the CC.

A non-linear association between amyloid burden and WM tract microstructure has been described previously.^{3,12} Although the study of Wolf et al. observed this relationship only at the global level, a recent study from Dong et al. showed regional diffusion changes depending on the amount of global amyloid burden, most prominently in the genu of the CC. However, within this study, the continuous amyloid burden was reduced to a dichotomous categorization. By including primarily early amyloid accumulators and using amyloid PET quantification as a continuous measure in this work, our results strongly support associations between regional amyloid- β ($A\beta$) deposition and regional disruptions in WM microstructure. More specifically, amyloid burden in the anterior cingulate cortex strongly related to AxD and RD measures of the genu of the CC, whereas amyloid burden in the precuneus related to MD measures in the body and FA measures in both the body and splenium of the CC. In addition, amyloid burden in the insula significantly related to FA measures of the cingulum. It is notable that these associations between amyloid burden and DTI measures showed statistically signifi-

cant dependence both with quadratic and linear fits. Thus, the behavior of DTI metrics as a function of increasing amyloid burden suggests that amyloid deposition might induce WM changes already in (very) early accumulating subjects. This observation is also supported by the recent work of Caballero et al. (2020), who showed that $A\beta$ deposition is associated with WM alterations throughout the adult lifespan.³⁵

Histological studies provide insight into the possible underlying processes of these *in vivo* observations. A recent study showed increased oligodendrocyte proliferation and remyelination of axons in early AD.³⁶ This could effectively hamper diffusion along the axons and thus result in altered DTI measures of diffusivity in subjects with early amyloid accumulation. In addition, Winklewski et al. (2018) reported acute axonal damage due to axonal swelling and fragmentation associated with an decrease in AxD, followed by microglial clearance of membrane fragments and decreased axonal density associated with an increase in AxD.³⁷ In accordance, initial RD decreases have been linked to axonal swelling during acute injury,³⁸ whereas subsequent RD increases are linked to demyelination.³⁷ In line with these histological observations, our results show an initial decrease in AxD and RD, followed by an increase in both metrics. Such non-linear patterns might entail multiple stages of axonal damage, which in light of recent literature might be explained as initial oligodendrocyte proliferation and axonal swelling upon low amyloid burden, followed by actual axonal degeneration only becoming apparent at a higher amyloid burden.³⁹ This also could explain why initial increases in WM FA were found not to be associated with cognitive decline in early AD, whereas decreases in WM FA were.^{3,5}

Non-linear associations between emerging amyloid pathology and imaging biomarkers might be able to capture the earliest response to amyloid deposition, arguably the first step of AD pathophysiological cascade.⁴⁰ In line with our work, a biphasic model of gray matter MD changes in asymptomatic subjects has been proposed.⁴¹ In addition, a trend toward larger hippocampal volume has been reported in subjects with intermediate amyloid burden compared to amyloid-negative subjects, whereas a loss of hippocampal volume was seen in clear amyloid-positive subjects.¹² Finally, recent work showed that elec-

troencephalography (EEG) patterns are modulated differently depending on the degree of amyloid burden, also in a non-linear fashion.⁴² Combining such imaging modalities showing biphasic response to amyloid deposition could further improve our understanding of the development of AD in its preclinical stages. Literature suggests that WM tract microstructure measures specifically of the CC^{12,43} seem to be promising early stage AD biomarkers in addition to amyloid pathology, and might support the identification of more accurate subject-specific disease trajectories. This could in turn improve risk-profiling efforts of preclinical AD subjects, and possibly support targeted inclusion for secondary prevention trials focusing on secondary prevention. Longitudinal studies are necessary to further validate this cross-sectional work and to investigate the value of combining regional WM integrity and amyloid burden measures in predicting cognitive decline.

Some methodological considerations of the current work should be addressed. First, we did not investigate associations between late amyloid accumulation regions and WM tracts, possibly missing other regional associations. In addition, the use of bilateral and tract-wise WM ROIs might overlook local effects. Voxel-wise association studies could avoid these limitations, and future work should investigate the possible added value of these approaches. Tract-level data might also have suffered from partial-volume effects (PVEs), that is, contamination of diffusion signals by cerebrospinal fluid. Thin WM bundles are especially vulnerable to PVE, resulting in underestimation of DTI metrics alterations in the smaller tracts. PVE might therefore explain the limited amount of associations in the thin cingulum bundles, while strong results were found in the larger body CC.⁴⁴ In addition, although the use of the skeletonized data for ROI extraction was chosen for its improved ability to detect subtle changes in the CC and tracts neighboring the ventricles, it might have been suboptimal for other WM tracts located more in the deep WM.³² Finally, the number of amyloid-positive subjects in this cohort is relatively low compared to previous literature (14% vs. \approx 20%),⁴⁵ given the average age of the study participants. This is probably because our apolipoprotein E (APOE) ϵ 4 carriers, which are at the highest risk of accumulating amyloid, are mostly in the 60- to 70-year age range (data not shown) and less likely to have high global amyloid burden, but rather are on the disease trajectory toward amyloid positivity.⁴⁶ Although continuous measures of amyloid burden were used, the low number of globally positive subjects may have limited the power to observe associations between regions known to be involved later in the amyloid accumulation process and more associative tracts like the SLF, considering the trend level associations already observed between global amyloid burden and SLF FA in this work.

5 | CONCLUSION

Regional amyloid burden is associated with disruption of the WM microstructure in cognitively unimpaired subjects. This association was driven mostly by amyloid burden in the precuneus and it could be most robustly measured in the body of the CC, where a non-

linear biphasic relationship between DTI metrics and amyloid burden was apparent. Our results might reflect initial amyloid-associated compensatory mechanisms of the WM, followed by axonal degeneration patterns in the earliest stages of AD. Taken together, DTI measures of the body of the CC are promising early AD biomarkers and could, together with amyloid burden, support risk-profiling efforts in preclinical AD subjects.

ACKNOWLEDGMENTS

The authors want to thank all PreclinAD participants for their efforts to join and complete this demanding study and our colleagues of The Netherlands Twin Register for referring participants. The research leading to these results has received support from the Innovative Medicines Initiative Joint Undertaking under European Medical Information Framework (EMIF) grant agreement No. 115372, resources of which are composed of financial contribution from the European Union's Seventh Framework Programme (FP7/2007-2013) and European Federation of Pharmaceutical Industries and Associations (EFPIA) companies in-kind contribution. The project leading to this paper has received funding from the Innovative Medicines Initiative 2 Joint Undertaking under Amyloid Imaging to Prevent Alzheimer's Disease (AMYPAD) grant agreement No. 115952 and European Prevention of Alzheimer's Dementia (EPAD) grant No. 115736. This Joint Undertaking receives the support from the European Union's Horizon 2020 Research and Innovation Programme and EFPIA. Frederik Barkhof is supported by the National Institute for Health Research University College London Hospitals (NIHR UCLH) Biomedical Research Centre. This work also received in-kind sponsoring of the PET-tracer from General Electric (GE) Healthcare. *This communication reflects the views of the authors and neither IMI nor the European Union and EFPIA are liable for any use that may be made of the information contained herein.*

AUTHOR CONTRIBUTIONS

L.E. Collij S. Ingala, H. Top, V. Wottschel, K. Stickney, J. Tomassen, E. Konijnenberg, M. Ten Kate, C. Sudre, I. Lopes Alves, M.M. Yaqub, A.M. Wink, and D. Van 't Ent report no disclosures relevant to the manuscript. P. Scheltens received grants from GE Healthcare, Piramal, and Merck, paid to his institution; he has received speaker's fees paid to the institution Alzheimer Center, VU University Medical Center, Lilly, GE Healthcare, and Roche. B.N.M. van Berckel reports no disclosures relevant to the manuscript. P.J. Visser has served as member of the advisory board of Roche Diagnostics. Dr Visser received nonfinancial support from GE Healthcare, research support from Biogen, and grants from Bristol-Myers Squibb, EU/EFPIA Innovative Medicines Initiative Joint Undertaking, and EU Joint Programme–Neurodegenerative Disease Research (JPND and ZonMw). F. Barkhof received payment and honoraria from Bayer Genzyme, Biogen-Idec, TEVA, Merck, Novartis, Roche, IXICO Ltd, GeNeuro, and Apitope Ltd for consulting; payment from the IXICOLtd, and MedScape for educational presentations; research support via grants from EU/EFPIA Innovative Medicines Initiative Joint Undertaking (AMYPAD consortium), EuroPOND (H2020), UK MS Society, Dutch MS Society, PICTURE (IMDI-NWO),

NIHR UCLH Biomedical Research Centre (BRC), and ECTRIMS-MAGNIMS. A. Den Braber reports no disclosures relevant to the manuscript.

REFERENCES

- Jack CR Jr., Knopman DS, Jagust WJ, et al. Tracking pathophysiological processes in Alzheimer's disease: an updated hypothetical model of dynamic biomarkers. *Lancet Neurol.* 2013;12:207-216.
- Clerx L, Visser PJ, Verhey F, Aalten P. New MRI markers for Alzheimer's disease: a meta-analysis of diffusion tensor imaging and a comparison with medial temporal lobe measurements. *J Alzheimers Dis.* 2012;29:405-429.
- Wolf D, Fischer FU, Scheurich A, Fellgiebel A. Alzheimer's disease neuroimaging I. non-linear association between cerebral amyloid deposition and white matter microstructure in cognitively healthy older adults. *J Alzheimers Dis.* 2015;47:117-127.
- Rieckmann A, Van Dijk KR, Sperling RA, Johnson KA, Buckner RL, Hedden T. Accelerated decline in white matter integrity in clinically normal individuals at risk for Alzheimer's disease. *Neurobiol Aging.* 2016;42:177-188.
- Vipin A, Ng KK, Ji F, Shim HY, et al. Amyloid burden accelerates white matter degradation in cognitively normal elderly individuals. *Hum Brain Mapp.* 2019;40:2065-2075.
- Molinuevo JL, Ripolles P, Simo M, et al. White matter changes in preclinical Alzheimer's disease: a magnetic resonance imaging-diffusion tensor imaging study on cognitively normal older people with positive amyloid beta protein 42 levels. *Neurobiol Aging.* 2014;35:2671-2680.
- Racine AM, Adluru N, Alexander AL, et al. Associations between white matter microstructure and amyloid burden in preclinical Alzheimer's disease: a multimodal imaging investigation. *Neuroimage Clin.* 2014;4:604-614.
- Palmqvist S, Scholl M, Strandberg O, et al. Earliest accumulation of beta-amyloid occurs within the default-mode network and concurrently affects brain connectivity. *Nat Commun.* 2017;8:1214.
- Grothe MJ, Barthel H, Sepulcre J, et al. In vivo staging of regional amyloid deposition. *Neurology.* 2017;89:2031-2038.
- Farrell ME, Chen X, Rundle MM, Chan MY, Wig GS, Park DC. Regional amyloid accumulation and cognitive decline in initially amyloid-negative adults. *Neurology.* 2018;91(19):e1809-e1821.
- Collij L, Konijnenberg E, Reimand J, et al. Assessing Amyloid pathology in cognitively normal subjects using [(18)F]Flutemetamol PET: comparing visual reads and quantitative methods. *J Nucl Med.* 2018;60(4):541-547.
- Dong JW, Jelescu IO, Ades-Aron B, et al. Diffusion MRI biomarkers of white matter microstructure vary nonmonotonically with increasing cerebral amyloid deposition. *Neurobiol Aging.* 2020;89:118-128.
- Thal DR, Beach TG, Zhanette M, et al. [(18)F]flutemetamol amyloid positron emission tomography in preclinical and symptomatic Alzheimer's disease: specific detection of advanced phases of amyloid-beta pathology. *Alzheimers Dement.* 2015;11:975-985.
- Villeneuve S, Rabinovici GD, Cohn-Sheehy BI, et al. Existing Pittsburgh Compound-B positron emission tomography thresholds are too high: statistical and pathological evaluation. *Brain.* 2015;138:2020-2033.
- Mattsson N, Palmqvist S, Stomrud E, Vogel J, Hansson O. Staging beta-Amyloid pathology with amyloid positron emission tomography. *JAMA Neurol.* 2019;76(11).
- Bischof GN, Jacobs HIL. Subthreshold amyloid and its biological and clinical meaning: long way ahead. *Neurology.* 2019;93(2):72-79.
- Willemsen G, Vink JM, Abdellaoui A, et al. The Adult Netherlands Twin Register: twenty-five years of survey and biological data collection. *Twin Res Hum Genet.* 2013;16:271-281.
- Konijnenberg E, Carter SF, Kate M Ten, et al. The EMIF-AD PreclinAD study: study design and baseline cohort overview. *Alzheimers Res Ther.* 2018;10: 75.
- Heeman F, Yaqub M, Lopes Alves I, et al. Optimized dual-time-window protocols for quantitative [(18)F]flutemetamol and [(18)F]florbetaben PET studies. *EJNMMI Res.* 2019;9: 32.
- Lammertsma AA, Hume SP. Simplified reference tissue model for PET receptor studies. *Neuroimage.* 1996;4:153-158.
- Boellaard R, Yaqub M, Lubberink M, Lammertsma A. PPET: a software tool for kinetic and parametric analyses of dynamic PET studies. *Neuroimage.* 2006;31: T62.
- Buckley CJ, Sherwin PF, Smith AP, Wolber J, Weick SM, Brooks DJ. Validation of an electronic image reader training programme for interpretation of [18F]flutemetamol beta-amyloid PET brain images. *Nucl Med Commun.* 2017;38:234-241.
- Desikan RS, Segonne F, Fischl B, et al. An automated labeling system for subdividing the human cerebral cortex on MRI scans into gyral based regions of interest. *Neuroimage.* 2006;31:968-980.
- Collij LE, Heeman F, Salvado G, et al. Multi-tracer model for staging cortical amyloid deposition using PET imaging. *Neurology.* 2020.
- Mattsson N, Palmqvist S, Stomrud E, Vogel J, Hansson O. Staging β -amyloid pathology with amyloid positron emission tomography. *JAMA neurology.* 2019;76:1319-1329.
- Fantoni E, Collij L, Alves IL, Buckley C, Farrar G. The spatial-temporal ordering of amyloid pathology and opportunities for PET imaging. *J Nucl Med.* 2019.
- Sudre CH, Cardoso MJ, Bouvy WH, Biessels GJ, Barnes J, Ourselin S. Bayesian model selection for pathological neuroimaging data applied to white matter lesion segmentation. *IEEE Trans Med Imaging.* 2015;34:2079-2102.
- Ten Kate M, Sudre CH, den Braber A, et al. White matter hyperintensities and vascular risk factors in monozygotic twins. *Neurobiol Aging.* 2018;66:40-48.
- Smith SM, Jenkinson M, Woolrich MW, et al. Advances in functional and structural MR image analysis and implementation as FSL. *Neuroimage.* 2004;23(Suppl 1): S208-19.
- Smith SM, Jenkinson M, Johansen-Berg H, et al. Tract-based spatial statistics: voxelwise analysis of multi-subject diffusion data. *Neuroimage.* 2006;31:1487-1505.
- Mori S, Oishi K, Jiang H, et al. Stereotaxic white matter atlas based on diffusion tensor imaging in an ICBM template. *Neuroimage.* 2008;40:570-582.
- Zhang S, Arfanakis K. White matter segmentation based on a skeletonized atlas: effects on diffusion tensor imaging studies of regions of interest. *J Magn Reson Imaging.* 2014;40:1189-1198.
- Minica CC, Dolan CV, Kampert MM, Boomsma DI, Vink JM. Sandwich corrected standard errors in family-based genome-wide association studies. *Eur J Hum Genet.* 2015;23:388-394.
- Pan W. Akaike's information criterion in generalized estimating equations. *Biometrics.* 2001;57:120-125.
- Caballero MAA, Song Z, Rubinski A, et al. Age-dependent amyloid deposition is associated with white matter alterations in cognitively normal adults during the adult life span. *Alzheimers Dement.* 2020.
- Mathys H, Davila-Velderrain J, Peng Z, et al. Single-cell transcriptomic analysis of Alzheimer's disease. *Nature.* 2019;570:332-337.
- Winklewski PJ, Sabisz A, Naumczyk P, Jodzio K, Szurawska E, Szarmach A. Understanding the physiopathology behind axial and radial diffusivity changes-what do we know?. *Front Neurol.* 2018;9: 92.
- Chu Z, Wilde EA, Hunter JV, et al. Voxel-based analysis of diffusion tensor imaging in mild traumatic brain injury in adolescents. *AJNR Am J Neuroradiol.* 2010;31:340-346.
- Wang Q, Wang Y, Liu J, et al. Quantification of white matter cellularity and damage in preclinical and early symptomatic Alzheimer's disease. *Neuroimage Clin.* 2019;22:101767.

40. Jack CR Jr., Bennett DA, Blennow K, et al. NIA-AA Research Framework: toward a biological definition of Alzheimer's disease. *Alzheimers Dement*. 2018;14:535-562.
41. Montal V, Vilaplana E, Alcolea D, et al. Cortical microstructural changes along the Alzheimer's disease continuum. *Alzheimers Dement*. 2018;14:340-351.
42. Gaubert S, Raimondo F, Houot M, et al. EEG evidence of compensatory mechanisms in preclinical Alzheimer's disease. *Brain*. 2019;142:2096-2112.
43. Lo Buono V, Palmeri R, Corallo F, et al. Diffusion tensor imaging of white matter degeneration in early stage of Alzheimer's disease: a review. *Int J Neurosci*; 2019: 1-8.
44. Oishi K, Lyketsos CG. Alzheimer's disease and the fornix. *Front Aging Neurosci*. 2014;6: 241.
45. Jansen WJ, Ossenkoppele R, Knol DL, et al. Prevalence of cerebral amyloid pathology in persons without dementia: a meta-analysis. *JAMA*. 2015;313:1924-1938.
46. Lopresti BJ, Campbell EM, Yu Z, et al. Influence of apolipoprotein-E genotype on brain amyloid load and longitudinal trajectories. *Neurobiol Aging*. 2020;94:111-120.

SUPPORTING INFORMATION

Additional supporting information may be found online in the Supporting Information section at the end of the article.

How to cite this article: Collij LE, Ingala S, Top H, et al. White matter microstructure disruption in early stage amyloid pathology. *Alzheimer's Dement*. 2021;13:e12124.
<https://doi.org/10.1002/dad2.12124>